

A Backscatter Imaging and Light Scattering System for Monitoring of Crystallization Processes

Amir Naqwi¹, Chris Fandrey¹, Gerry Kauma¹,
David Grant², Yushi Feng², and Sachin Lohani²

1: Powerscope Inc., 1313 Fifth St. SE, Suite 209, Minneapolis, MN 55414, USA, info@powerscopetech.com

2: Department of Pharmaceutics, University of Minnesota, 308 Harvard St. SE, Minneapolis, MN 55455, USA

Abstract A miniature optical probe (16 mm in diameter and 300 mm length) is developed for diagnostics of crystallization processes. A probe volume is produced near the optical window at the end of the cylindrical probe. The probe volume consists of a CW laser beam spot of about 50 micron diameter, which is viewed by a photodetector. Crystals crossing an ellipsoidal region of 50 μm diameter and 100 μm length scatter CW light into the photodetector. Increase in the photodetector output (caused by the light scattered off a crystal) triggers a camera and a pulsed laser. The pulsed laser spot size and the camera viewing area are significantly larger (~500 μm in diameter) than the CW spot size, so the crystals are fully illuminated and imaged. Multimode optical fibers are used to bring the CW light and the pulsed laser light to the end of the cylindrical probe. A multimode fiber and an imaging fiber bundle are used to collect the scattered CW light and the crystal image respectively. A thermistor is also located at the end of the probe for monitoring the crystallizer temperature. All the measured data is transferred to a computer via IEEE 1394. A software displays images in real-time and is capable of post-processing and displaying data in various forms, such as correlation between crystal size and temperature. Measurements of a crystallization process have shown that the sudden growth of crystallization nuclei is accompanied by a rise in the solution temperature due to the heat of crystallization. Further, correlation between the measured crystal size and the aspect ratio is used to predict the three-dimensional structure (habit) of the crystals. In the results reported here, a positive correlation is found, *i.e.* aspect ratio increases with the effective particle size. This correlation is indicative of rod-like crystals. A negative correlation is expected for plate-like crystals. In-situ determination of crystal habit is valuable in pharmaceutical applications; e.g. plate-like crystals are suitable for making drug tablets as they provide larger area for adhesion.

1. Introduction

This work is primarily concerned with the monitoring and control of the pharmaceutical crystallization processes. Most drug substances in the pharmaceutical industry are purified by crystallization from solution (Mullin 1993). The crystal size and shape (habit) can be easily affected by the crystallization conditions, such as cooling rate, turbulence level etc. The crystal habit in turn influences the efficiency of crystallization (Mullin 1993).

It is desirable in pharmaceutical manufacturing to produce crystals with an optimal size, as very small crystals are hard to separate from the liquid; *i.e.* filtration time may be unduly long. On the other hand, large crystals generally have poor mechanical compaction and thermodynamic properties (Bandyopadhyay 1998 and Sun & Grant 2001). They tend to absorb excessive amounts of impurities (Zhang & Grant 1999 and Gu & Grant 2000) and contain undesirable liquid inclusions that cause caking of the final product.

Crystal shape is also important as it affects the powder properties. Recent studies have shown that plate-like crystals have improved mechanical compaction properties over prism-shaped and needle-shaped crystals (Bandyopadhyay 1998 and Sun & Grant 2001) and hence have better tableting performance. Other processes, succeeding crystallization, that are affected by the particle size and shape are pneumatic transport of the crystals (Yin et al. 1986), suspensions formulation

(Tiwary & Panpalia 1999), filling of tableting die (Ridgway & Scotton 1970) and bulk solid handling (Pitkin & Carstensen 1990).

Hence, availability of an instrument for in-situ crystal size and shape measurement will enhance the performance and quality of subsequent process steps.

In-situ crystal measurement will also complement on-going work on the crystallization mechanisms of conventional and modern materials. Efforts have been devoted to specifying the desirable crystal habits for various applications (Haleblian 1975 and York 1983). There have also been efforts to micro-control the size and shape of crystals (Lahay & Leiserowitz 1993 and Winn & Doherty 1998).

Furthermore, there have been substantial developments on theoretical modeling of the crystal size distribution (CSD). A summary of this work is given below to highlight the importance of a complementary experimental method for in-situ measurement of CSD.

The continuous mixed suspension, mixed product removal (CMSMPR) mode of crystallization is easier to model and was originally addressed by the modelers; however, batch crystallization mode has distinct advantages in terms of operating cost, material quantities, and flexibility of operating conditions (Tavare 1987). Theoretical models of CSD in a batch crystallizer have been based on either a stochastic framework (Fan et al. 1987, Hsu & Fan 1987 and Hsu et al. 1988) or a deterministic framework (Rawling et al. 1993) that incorporates a single stochastic variable to account for the measurement variability and noise.

A typical model consists of a differential equation that expresses the nucleation and crystal growth rate as a linear function of the degree of supersaturation raised to some constant power. After solving the differential equation (which may be done in Laplace domain, see Tavare & Garside 1986), one ends up with several unknown coefficients that are shown to depend upon the details of the crystallizer geometry (see e.g. Shimizu et al. 1995) and operating conditions. Several authors have considered using experimental data to determine the unknown coefficients (see Rawling et al. 1993, Garside et al. 1988, Qiu & Rasmuson 1991 and Dash & Rohani 1993). In this respect, an instrument for time-resolved in-situ measurement of CSD is obviously a powerful tool at the disposal of the modelers.

In order to address the needs discussed above, a backscatter imaging particle analyzer (BIPA) is developed and packaged in a miniature optical probe (16 mm in diameter) as described below.

2. Measurement System

The cylindrical probe has an optical window at the end. The optical probe volume is produced very close to this window, in order to make sure that the first crystal next to the window is measured. As shown in Figure 1, a CW laser beam is focused to a spot of about 50 micron, which is viewed by the photodetector (an avalanche photodiode). A small detection volume is formed, which is shown in gray. When a crystal arrives in the detection volume, photodetector output increases, which triggers a camera and a pulsed laser. The pulsed laser spot size and the camera viewing area are significantly larger (~500 μm) than the detection volume, so the crystals are fully illuminated and imaged.

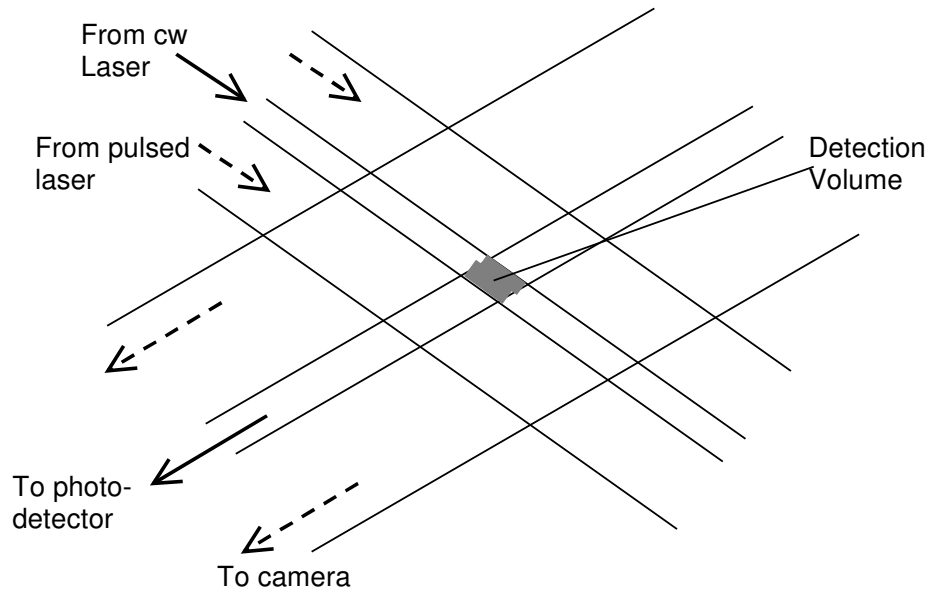


Figure 1: Probe volume

Multimode optical fibers are used to bring the CW light and the pulsed laser light to the end of the cylindrical probe. A multimode fiber and an imaging fiber bundle are used to collect the scattered CW light and the crystal image respectively. A thermistor is also located at the end of probe for monitoring the crystallizer temperature. All the fiber links and electrical leads of the thermistor terminate in a control box, which houses lasers, photodetector, camera, thermistor bridge and the processing electronics. Light scattering, imaging and temperature data are sent out of the control box via Firewire to a computer. A Windows™ software is used to display the images and other data. Particle images are processed in real time and their characteristics (size and aspect ratio) are displayed and saved by the software.

As shown in Figure 2, Pulses A1 coming from APD indicate the transit of a particle in the measurement volume. The electronic system generates a trigger TG1 based on the user-specified threshold Th1. It also measures the transit time based on the user specified thresholds Th1 and Th2. Transit time output is a 24 bit integer representing the clock cycle of 128 ns; i.e. resolution of transit time is 128 ns and the largest measurable value is about 2 s. Typical particle transit times in a crystallizer are order of milliseconds. Hence, the above range and resolution are satisfactory.

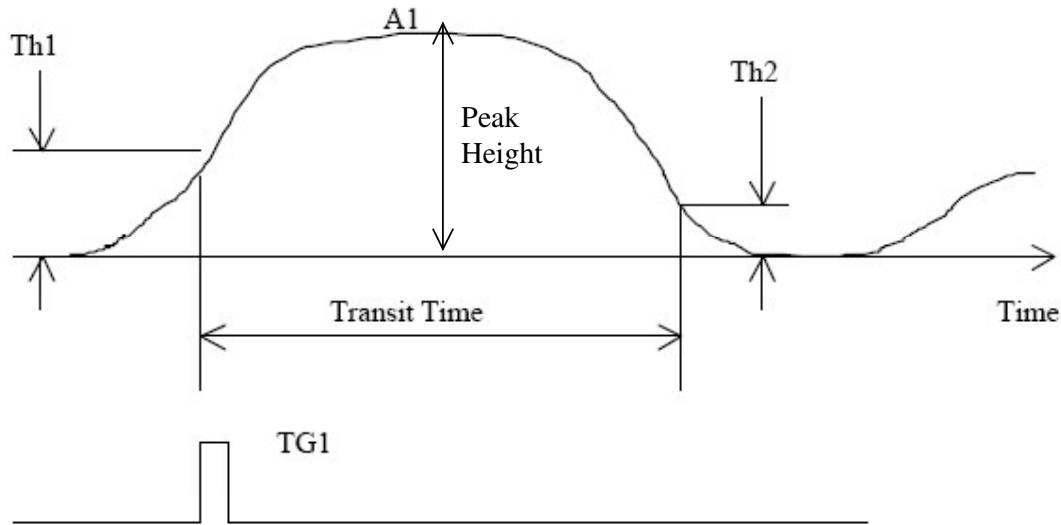


Figure 2: Relationship of the APD signal and the pulse to trigger laser

Events starting TG1 are as follows:

1. System electronics routes TG1 to the camera. The camera integration time is set long enough to cover the laser pulse (15–300 ns).
2. After a delay (~100 ns), the electronics sends a TTL signal to fire the pulsed laser. The laser pulse width is chosen by the user and lasts 15–300 ns.
3. A frame is grabbed from the camera. If frame is not available, the no-frame flag is set.
4. The thermistor reading is digitized.
5. The data package (camera frame + thermistor reading + transit time + peak height + time stamp + no-frame flag + missed particle transit time + missed particle peak height) is sent to the computer. The no-frame flag is reset.

The hardware system recognizes that it may not be possible to grab a frame for each particle due to the limited frame rate of the camera (~1000 frames/second). However, it would be generally possible to measure the transit time and peak height of each particle as the photodetector response is very fast. The electronic system is built in such a way that we do not miss any particles that arrive during frame transfer.

The basic monitoring of the APD and capturing of an image are controlled by the Digital Signal Processing (DSP) chip, which is a Field Programmable Gate Array. An image can be captured in one of the following operating modes:

1. Free running mode: camera grabbing frames continuously at the maximum rate;
2. A single frame capture based on a command from the computer;
3. Triggered mode: frame is captured when the APD signal crosses a programmable threshold.

These features make BIPA a versatile measurement system.

3. Applications

BIPA probe can be used in a full-scale crystallizer as well as a laboratory-scale crystallization experiment. An example of a laboratory experiment is shown in Figure 3. A small jacketed vessel is used to grow lysine monohydrochloride crystals out of a 1:1 mixture of water and methanol.

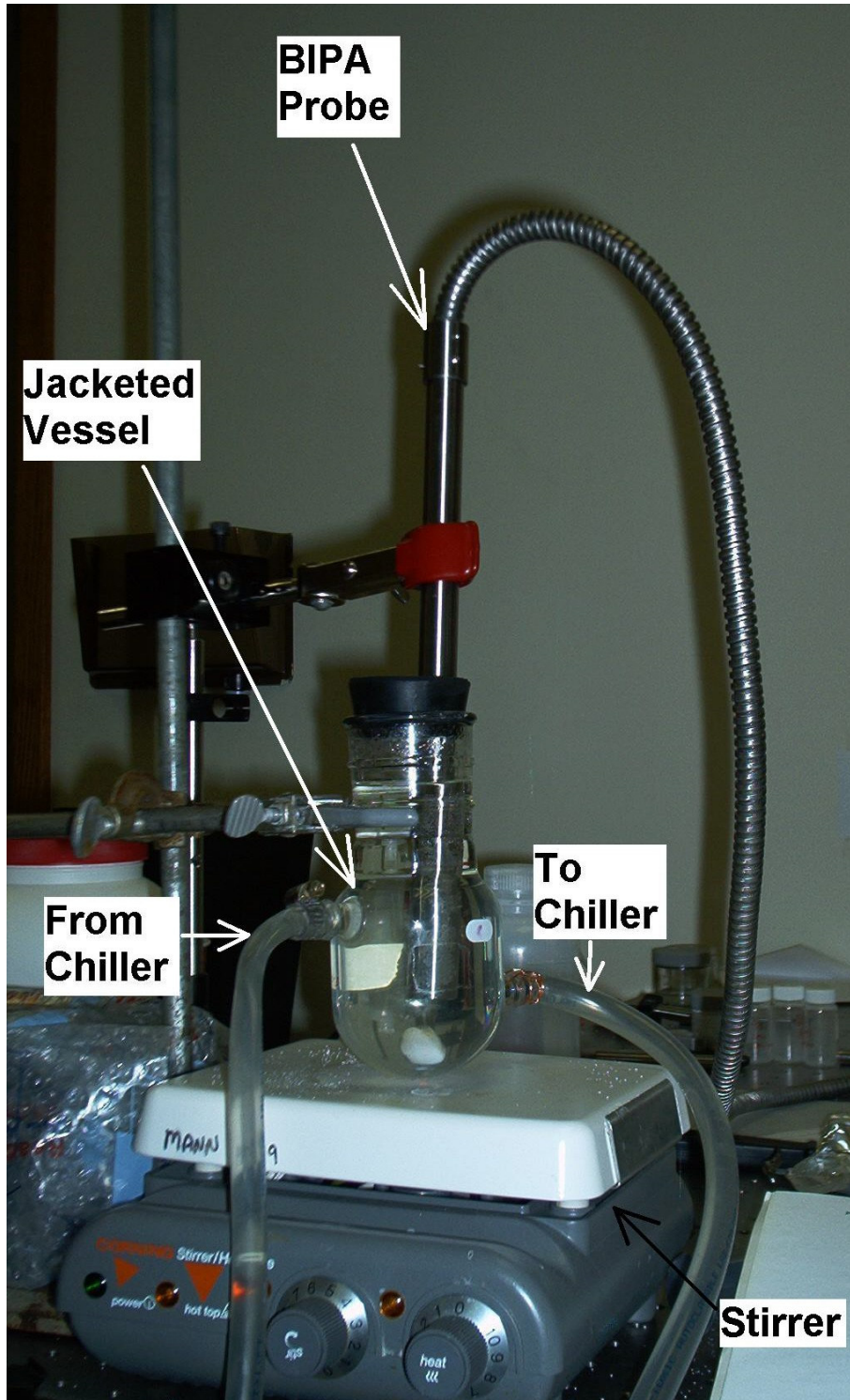


Figure 3: A laboratory-scale crystallization experiment using the miniature probe

We kept the solution at a high temperature for a while to ensure that all the crystallization nuclei were fully dissolved. It was slowly cooled down to the saturation temperature by lowering the temperature of water in the cooling jacket. The solution was placed on a magnetic stirrer and was constantly stirred using a magnetic ‘fish’. At the saturation temperature, crystal size grew

quickly and temperature increased by about 5 degrees, as shown in Figure 4. The heat of crystallization caused the rise in temperature.

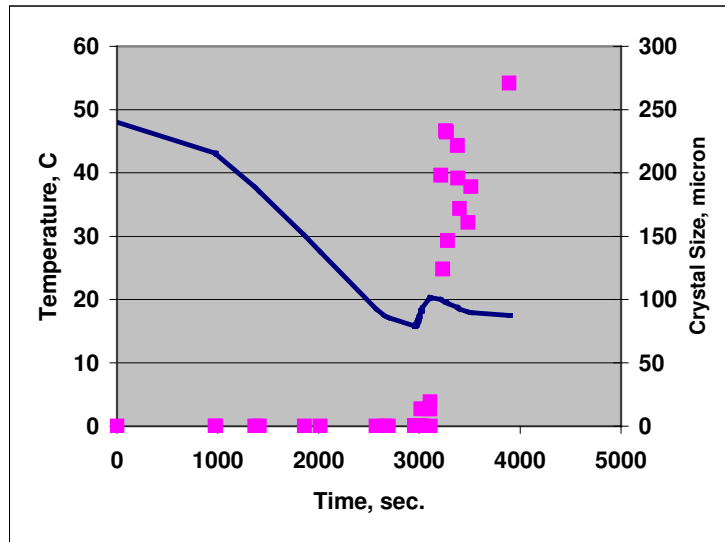


Figure 4: Crystallizer temperature and the crystal size as a function of time

Another series of experiments were conducted with lysine monohydrochloride crystals suspended in 111-trichloroethane, which does not dissolve them. Various solid volume fractions were measured. These measurements show that the transit time provides a good measure of solid volume fraction. Volume fraction near the probe agrees well with the bulk volume fraction if it is smaller than 1%. For dense suspensions, a region of low particle concentration is formed near the window.

Above measurements also show that it is possible to use two-dimensional images to infer the three-dimensional structure of pharmaceutical crystals, which are generally divided into three classes: plate-like, rod-like or prism-like (or rounded). In the case of plate-like crystals, there is a negative correlation between the size and the aspect ratio based on the two-dimensional images. This correlation is positive for the rod-like crystals, whereas no correlation is found for rounded crystals. Figure 5 shows the correlation for the above experiments depicting that these crystals are rod-like, which was verified by microscopic observations.

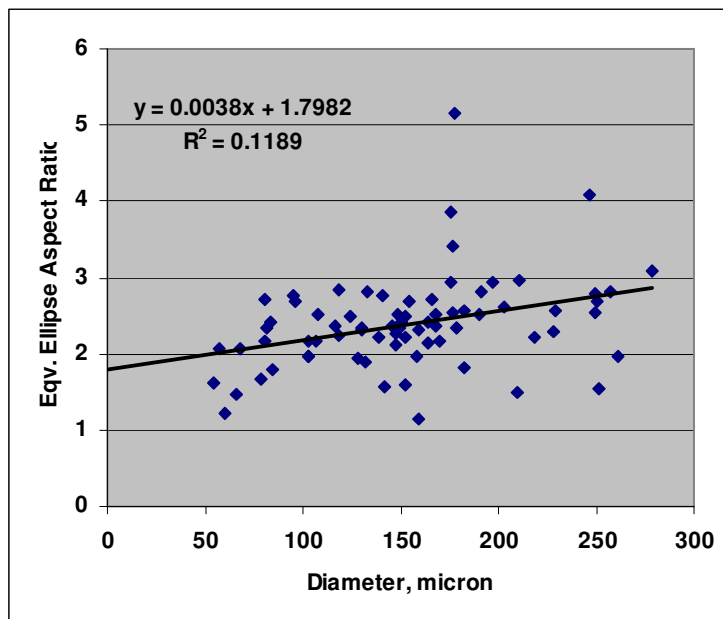


Figure 5: Aspect ratio versus crystal size (Equivalent Diameter) validating rod-like crystal structure

4. Conclusion

A multi-purpose measurement system is reported for the investigation of crystallization processes. A miniature probe is used to obtain simultaneous measurements of particle image, particle transit time and the backscatter signal strength. It also monitors the local temperature. Chemically resistant materials are used, so the probe can be used in a variety of pharmaceutical and chemical processes. This system is suitable for both the laboratory and manufacturing applications. Two-dimensional particle images are shown to be useful for a broad classification of the crystals into plate-like, rod-like and prism-like crystals.

Acknowledgement:

This work was funded by the National Institutes of Health, Grant # 5R44GM062072, Program Official: Charles G. Edmonds

References

- Bandyopadhyay R (1998) Influence of crystal properties on the tableting behavior of Lysine derivatives, Ph. D. Dissertation. University of Minnesota
- Dash SR, Rohani S (1993) Iterative parameter estimation for extraction of crystallization kinetics of potassium chloride from batch experiments. *Can. J. Chem. Eng.* 71(4): 539–548
- Fan LT, Chou ST, Hsu JP (1987) Transient analysis of crystallization: effect of size-dependent residence time of classified product removal. *AIChE Symp. Ser.* 83(253): 120–129
- Garside JL, Gibilaro G, Tavare NS (1988) Evaluation of crystal growth kinetics from a desupersaturation curve using initial derivatives. *Chem. Eng. Sci.* 43: 69–77
- Gu CH, Grant DJW (2000) Effects of crystallization in the presence of the diastereomer impurity on the crystal properties of (SS)-(+)-pseudoephedrine hydrochloride. *Enantiomer*, 5: 271–280
- Haleblian JK (1975) Characterization of habits and crystalline modification of solids and their pharmaceutical applications. *J. Pharm. Sci.*, 64: 1269–1288

- Hsu JP, Fan LT (1987) Transient analysis of crystallization: effect of size-dependent growth rate. *Chem. Eng. Commun.* 56: 19–40
- Hsu JP, Fan LT, Chou ST (1988) Transient analysis of crystallization: effect of initial size distribution. *Chem. Eng. Commun.* 69: 95–114
- Lahav M, Leiserowitz L (1993) Tailor-made auxiliaries for the control of nucleation, growth and dissolution of two- and three-dimensional crystals. *J. Physics D. Appl. Phys.* 26: B22-B31
- Mullin (1993) *Crystallization*, 3rd Edn. Butterworth-Heinemann, London
- Pitkin C, Carstensen JT (1990) Effect of particle shape on some bulk solids properties. *Drug Dev. Ind. Pharm.* 16: 1–12
- Qiu Y, Rasmuson AC (1991) Nucleation and growth of succinic acid in a batch cooling crystallizer. *AIChE J.* 37: 1293–1304
- Rawling JB, Miller SM, Witkowski WR (1993) Model identification and control of solution crystallization processes: a review. *Ind. Eng. Chem. Res.* 32: 1275–1296
- Ridgway K, Scotton JB (1970) The effect of particle shape on the variation of fill of a tableting die. *J. Pharm. Pharmac.* 22 Suppl: 24S–28S
- Shimizu K, Nagasawa H, Takahasi K (1995) Effect of off-bottom clearance of a turbine type impeller on crystal size distribution of aluminum potassium sulfate in a batch crystallizer. *J. Crystal Growth*, 154: 113–117
- Sun C, Grant DJW (2001) Influence of crystal shape on the tableting performance of L-Lysine Monohydrochloride Dihydrate. *J. Pharm. Sci.* 90: 567–579
- Tavare NS (1987) Batch crystallizers: a review. *Chem. Eng. Commun.*, 61: 259–318
- Tavare NS, and Garside J (1986) Simultaneous estimation of crystal nucleation and growth kinetics from batch experiments. *Chem. Eng. Res. Des.* 64: 109–118
- Tiwary AK, Panpalia GM (1999) Influence of crystal habit on trimethoprim suspension formulation. *Pharm. Res.* 16: 261–265
- Winn D, Doherty MF (1998) A new technique for predicting the shape of solution-growth organic crystals. *AIChE J.* 44: 2501-2514
- Yin MJ, Beddow JK, Vetter AF (1986) Effects of particle shape on two-phase flow in pipes. *Powder technology.* 46: 53–60
- York P (1983) Solid-state properties of powders in the formulation and processing of solid dosage forms. *Int. J. Pharm.*, 14: 1–28
- Zhang GGZ, Grant DJW (1999) Incorporation mechanism of guest molecules in crystals: solid solution or inclusion? *Intl. J. Pharmaceutics*, 181: 61–70